Frontiers in Health Informatics
ISSN-Online: 2676-7104
www.healthinformaticsjournal.com
2024; 13: 03
Open Access

Development and Characterization of Naftifine- Loaded Nanoemulsion-Based Nanogels: A Promising Approach for Antifungal Drug Delivery

Swapnil Deelip Phalak[1], Ramenani Hari Babu[2], Parminderjit Kaur[3*], Harish R. Pawar[4], B Nagarani[5], J.Sangeetha[6], Vema Kiran[7], Touseef Begum[8]

[1]Department of Pharmaceutics, Konkan Gyanpeeth Rahul Dharkar College of Pharmacy and Research Institute Karjat Dist- Thane Maharashtra Pin Code-410201.
[2]Department of Pharmacy Practice, Teerthanker Mahaveer College of Pharmacy, Teerthanker Mahaveer University, Moradabad, Uttar Pradesh, India. 244001.
[3]Department of Pharmaceutics, Khalsa College of Pharmacy Amritsar Pin- 143001.
[4]Department of Pharmaceutical Chemistry, College of Pharmaceutical Sciences, PIMS (DU), Loni, Ahmednagar, Maharashtra- 413736.
[5]Department of Pharmaceutics, Srikrupa Institute of Pharmaceutical Sciences, Velikatta, Siddipet, Telangana-502277.
[6]Department of Pharmacognosy, Mallareddy Institute of Pharmaceutical Sciences, Maisammaguda, Dhulapally, Kompally, Secunderabad -500100
[7]MB School of Pharmaceutical Sciences, Mohanbabu University, Tirupati, Andhra pradesh-517102.
[8]Ibn Sina National College for Medical Studies, P.O. Box 31906, Jeddah 21418 Kingdom of Saudi Arabia.
Corresponding Author: Parminderjit Kaur[3*]
Department of Pharmaceutics, Khalsa College of Pharmacy Amritsar, Pin- 143001

Cite this paper as: Swapnil Deelip Phalak, Ramenani Hari Babu, Parminderjit Kaur, Harish R. Pawar, B Nagarani, J.Sangeetha, Vema Kiran, Touseef Begum (2024) Development and Characterization of Naftifine- Loaded Nanoemulsion-Based Nanogels: A Promising Approach for Antifungal Drug Delivery. *Frontiers in Health Informatics*, 13 (3),9909-9926

A B S T R A C T

This study explored the development of nanoemulsion-based nanogels for the enhanced delivery of Naftifine, an antifungal agent. Various formulations, including blank (F1), drug-loaded nanoemulsion (F2), and chitosan-based nanogel (F3), were prepared and evaluated for their physical and chemical properties. The nanoemulsions were prepared using olive oil, lecithin, and xanthan gum, followed by the incorporation of Naftifine into selected formulations. Chitosan nanogel was developed by mixing the nanoemulsion with a chitosan gel base. The formulations were characterized for viscosity, droplet size, surface charge, polydispersity index (PDI), and drug content. FTIR spectroscopy confirmed no interaction between Naftifine and the excipients. The antifungal efficacy of the formulations was assessed using Minimum Inhibitory Concentration (MIC) tests against Trichophyton rubrum and Microsporum canis. Results showed that the nanoemulsion-based nanogel exhibited superior drug release and antifungal activity compared to the nanoemulsion alone, indicating its potential for more effective antifungal therapy.

Keywords: *Naftifine, Nanoemulsion, Nanogel, Chitosan, Antifungal.*

INTRODUCTION

Nanoemulsions and nanogels are advanced drug delivery systems that offer unique advantages in pharmaceutical and cosmetic applications due to their small particle size and enhanced bioavailability. Nanoemulsions are colloidal systems consisting of nanoscale droplets, typically ranging from 20 to 200 nm, dispersed in a continuous phase (Krishnan-Natesan, 2009, Newland and Abdel-Rahman, 2009). These systems are stabilized by surfactants and offer improved solubility, stability, and controlled release of hydrophobic drugs. Nanoemulsions are widely used in topical, oral, and parenteral drug delivery because of their ability to enhance drug penetration through biological membranes, ensuring better therapeutic outcomes (Kaur et al., 2017, Kaur et al., 2019, Smoleński et al., 2021). Nanogels, on the other hand, are hydrogel-based formulations with a network structure that can encapsulate drugs within their matrix. These gel-like systems are typically composed of polymers like chitosan, and their size can range from 1 nm to 1000 nm. Nanogels offer excellent swelling properties, biocompatibility, and tunable mechanical strength, making them ideal for controlled or sustained drug release. Due to their higher viscosity compared to nanoemulsions, nanogels are particularly suited for localized drug delivery, such as transdermal patches or topical applications, where a slower release is beneficial (Patil et al., 2024, Ranjbar et al., 2023, Krishnan-Natesan, 2009). Both nanoemulsions and nanogels are promising platforms for the delivery of active ingredients, providing flexibility in formulation design, stability, and enhanced therapeutic efficacy. The rationale for preparing nanoemulsion-based nanogels of naftifine lies in the need to enhance the delivery and efficacy of this antifungal agent, commonly used for treating skin infections such as athlete's foot and ringworm. Naftifine, being lipophilic, faces challenges in solubility and penetration through the skin's hydrophobic barrier (Balfour and Faulds, 1992, Darkes et al., 2003, Leyden, 1998, Das et al., 2024). Nanoemulsions, with their nanoscale droplet size, offer a solution by improving drug solubility and promoting deeper skin penetration. These properties enhance naftifine's bioavailability at the site of infection, potentially reducing dosing frequency and improving therapeutic outcomes. Incorporating the nanoemulsion into a nanogel matrix further optimizes its application. Nanogels, with their gel-like consistency, provide a more controlled and sustained release of the drug. This ensures prolonged contact with the affected area, enhancing the drug's antifungal activity over time. Moreover, nanogels are easy to apply, offer superior spreadability, and are more comfortable for patients due to their non-greasy nature (Kothapalli et al., 2024, Szumała and Macierzanka, 2022, Donthi et al., 2022, Das et al., 2024). By combining the advantages of both nanoemulsions and nanogels, a nanoemulsion-based nanogel formulation of naftifine would offer enhanced drug delivery, improved patient compliance, and potentially superior clinical outcomes in the treatment of superficial fungal infections. This dual system aims to address both solubility and release challenges associated with naftifine (Newland and Abdel-Rahman, 2009, Jessup et al., 2000). To summarise, the creation of a nanogel formulation of Naftifine presents a promising strategy for treating fungal infections affecting the skin and nails. It may result in higher patient compliance, targeted distribution, delayed release, and enhanced effectiveness. As a result, the goal of the current work is to create nanogels of naptifine based on nanoemulsion and assess their different physicochemical characteristics and antifungal capabilities.

MATERIAL AND METHODS

Drugs and chemicals

The study utilized a variety of drugs and chemicals essential for the formulation of nanoemulsions and nanogels. The active drug used (Naftifine) was incorporated into the nanoemulsion (F2), with blank formulations (F1) serving as controls. Naftifine was received as gift sample from Arizon pharma, Himachal Pradesh. Chitosan was employed as a key polymer in the nanogel (F3) for its biocompatibility and gel-forming properties and was procured from Sigma Aldrich. Other excipients included surfactants, emulsifiers, and stabilizers to ensure the formulations' stability and effectiveness and were procured from reputed vendors. All chemicals used, including solvents and reagents for analysis, were of analytical grade.

Preparation of nanoemulsion (NEM)

The nanoemulsion was prepared using the previously described protocol (Zhou et al., 2016) with a few essential modifications. The prepared formulas are listed in Table 1 below. The nanoemulsions (NEM-1 to NEM-4) were prepared using a systematic approach. Initially, the oil phase was created by accurately weighing olive oil, lecithin, and the drug (for NEM-2 to NEM-4) according to the specified amounts in Table 1. These components were mixed thoroughly to ensure homogeneity of the oil phase. Simultaneously, the aqueous phase was prepared by weighing xanthan gum in the required quantity for each formulation and dissolving it in distilled water. Continuous stirring was applied to achieve complete dispersion of the xanthan gum in the water. Once both phases were ready, the oil phase was slowly introduced into the aqueous phase while stirring at a moderate speed of 500-1000 rpm. This step initiated the emulsification process. Following this, high-speed homogenization was carried out for a predetermined time to form a fine, uniform nanoemulsion. After emulsification, distilled water was added to each formulation to adjust the total weight to 100 g. The completed nanoemulsions were then transferred into sealed containers for further analysis and characterization, ensuring that the desired concentration of each component was accurately achieved in the final formulations.

Table 1. Table of formula composition for nanoemulsions with varying component amounts

Code for the formulations	Olive Oil (w/w)	Xanthan Gum (w/w)	Lecithin (w/w)	Drug (% w/w)	Distilled water Q. S to make 100 g
NEM-1 (Blank)	20 g	25 g	20 g	-	59 g
NEM-2	25 g	20 g	19 g	2%	41.75 g
NEM-3	22 g	23 g	17 g	2%	43.75 g
NEM-4	25 g	20 g	15 g	2%	45.75 g

Evaluation of nanoemulsions and preparation of chitosan gel

Several nanoemulsion formulations were physically inspected before being added to the gel matrix. We carefully monitored the colour shifts, homogeneity, and phase separation of the different formulations. For a period of 28 days, samples from each formulation were stored at 8°C, 25°C, 40°C, and 40°C with 75% relative humidity (RH). The chitosan gel was created by dissolving chitosan in distilled water. Using the procedure outlined by Zhou et al. (2016), a precise weight of 2.5 grammes of chitosan was measured and then dissolved in 100 millilitres

of distilled water containing 1.5% acetic acid (Zhou et al., 2016). To create the gel, a high-speed mixer running at 4000 rpm for 10 minutes was used. The resultant gel was then allowed to set overnight in storage prior to being mixed into the emulsion.

Making the nanogel for the nanoemulsion

For the chitosan gel preparation, chitosan was first dissolved in a 1% acetic acid solution under continuous stirring until a clear, homogeneous solution was obtained. Following this, the selected nanoemulsion was slowly added to the chitosan solution while maintaining stirring to ensure uniform distribution. The solution was then neutralized by adding a small amount of sodium hydroxide (NaOH) to promote gel formation, adjusting the pH to a skin-friendly range of 5.5 to 6.5. The mixture was stirred until a smooth gel was formed, after which it was stored in suitable containers for further evaluation. This method ensured that the formulations were both stable and effective, making them suitable for potential therapeutic applications.

Characterizations

Thermodynamic stability and Heat cooling cycle

The thermodynamic stability of the optimized formulations was assessed over 28 days, following the International Conference on Harmonisation (ICH) guidelines. This evaluation was conducted to determine how well the formulations could withstand adverse environmental conditions. Both the nanoemulsion (NEM) and the chitosan-based nanoemulsion gel (NEMG) were subjected to this test, using a method adapted from Burki et al. (2020), with some modifications (Burki et al., 2020).The formulations were first placed in an incubator at 40°C for 28 days. After this period, they were allowed to cool and return to room temperature. The purpose of this assessment was to identify any physical changes, such as the appearance of turbidity, creaming, or cracking, which could indicate formulation instability. Observing these changes helped evaluate the long-term stability of the formulations and their ability to endure thermal fluctuations, ensuring their viability for extended storage.

The cycle of freeze-thaw and centrifugation

The stability of both the nanoemulsion (NEM) and nanoemulsion gel (NEMG) formulations was further evaluated through a freeze-thaw cycle test, conducted over a period of 28 days. During this test, the formulations were placed in a deep freezer at a temperature between 2-4°C. After the freezing phase, they were removed and allowed to thaw at room temperature. Following each cycle, the formulations were visually examined to determine whether they had reverted to their original state, indicating physical stability.

In addition to the freeze-thaw test, a high-speed centrifugation test was performed using a Remi centrifuge (Remi, India). The formulations were placed in separate Eppendorf tubes and subjected to centrifugation at speeds of 6000 and 12000 rpm for 12 minutes each. This process was intended to evaluate the formulations' tendency to separate into oily and aqueous phases. Observations of phase separation provided important information on the overall stability and integrity of the emulsions, helping to confirm the robustness of the formulations under stress conditions.

The NEM and NEMG's pH, droplet size, surface charge, and PDI

The pH, droplet size, surface charge, and polydispersity index (PDI) of both the nanoemulsion (NEM) and the nanoemulsion gel (NEMG) were carefully analyzed to ensure the formulations' quality and stability (Burki et al., 2020). The pH of both NEM and NEMG was measured using

a calibrated pH meter to ensure compatibility with biological systems, particularly skin applications. The pH was expected to fall within an acceptable range, which is typically skin-friendly, ensuring that the formulations would not cause irritation. The droplet size of the formulations was assessed using dynamic light scattering (DLS) techniques. This parameter is crucial for nanoemulsions, as smaller droplet sizes generally contribute to better stability and more effective drug delivery. The average droplet size for both NEM and NEMG was measured and compared. The surface charge, or zeta potential, was evaluated to determine the stability of the emulsions. A higher absolute value of zeta potential suggests better stability due to increased repulsion between droplets, reducing the likelihood of aggregation (Ali et al., 2020). The zeta potential of both formulations was measured using a zeta potential analyzer. The polydispersity index (PDI) was also measured to evaluate the distribution of droplet sizes within the formulations. A lower PDI value indicates a more uniform distribution of droplet sizes, contributing to the stability and consistency of the nanoemulsion. Both NEM and NEMG were analyzed for PDI, with values expected to reflect a stable and uniform system (Ali et al., 2020). Together, these parameters provided a comprehensive evaluation of the formulations' stability, ensuring that they met the required standards for effective and safe application.

Analysis of the drug content

With only minor adjustments, the drug content analysis was carried out using the previously outlined approach (Burki et al., 2020). The drug content in the nanoemulsion gel (NEMG) formulations was analyzed to ensure the proper incorporation and consistency of the drug within each system. This was done by taking a specific amount of each formulation and diluting it with an appropriate solvent to dissolve the drug completely. The diluted samples were then subjected to UV-visible spectrophotometry, depending on the drug's characteristics and the method's sensitivity. Calibration curves were prepared using known concentrations of the drug to ensure accurate quantification. The absorbance or peak area obtained from the samples was compared to the calibration curve to determine the exact drug content. Each analysis was performed in triplicate to ensure accuracy and reproducibility. The drug content was then expressed as a percentage of the theoretical amount, and results within the acceptable range indicated that the drug had been uniformly incorporated into the formulations. Any significant deviation would suggest issues with the drug loading process or potential loss during formulation. This analysis ensured that the NEMG contained the desired drug concentration for therapeutic efficacy.

NEMG viscosity and morphological investigations

The viscosity of the nanoemulsion gel (NEMG) was measured to evaluate the flow properties and ensure that the gel had the appropriate consistency for topical application. The viscosity measurement was carried out using a viscometer, typically a Brookfield viscometer, at a controlled temperature to maintain accuracy (Alexander et al., 2013). The spindle speed and torque were adjusted based on the gel's characteristics. The viscosity values provide insights into the gel's ease of application, spreadability, and stability. A higher viscosity ensures that the formulation stays at the application site for an extended period, while lower viscosity may result in easier application but less retention on the skin. The results of the viscosity measurement helped to confirm the desired consistency of NEMG, suitable for its intended use. For morphological studies, the structure and shape of the droplets in both the nanoemulsion (NEM) and the nanoemulsion gel (NEMG) were analyzed using scanning electron microscopy (SEM) (El-Refaie et al., 2015). A small amount of the sample was placed on a grid or surface, and after necessary preparation, such as drying or staining, the samples were visualized under

high magnification. The SEM images provided detailed insights into the droplet size, shape, and surface characteristics of the formulations. The spherical morphology of the droplets, along with their uniform size distribution, indicated the successful formation of a stable nanoemulsion. Any deviations, such as irregular shapes or aggregated particles, would suggest instability or improper formulation. These morphological studies confirmed that both NEM and NEMG had uniform and consistent structures, contributing to their stability and effectiveness for drug delivery (El-Refaie et al., 2015, Burki et al., 2020).

FTIR spectroscopy: Drug excipient compatibility study

FTIR spectroscopy using a Perkin Elmer instrument was employed to evaluate the drug, chitosan, nanoemulsion, and nanoemulsion gel. The purpose of the study was to assess the compatibility between the polymer and other formulation components, as well as to identify functional groups and their respective wave numbers. Each sample, including individual ingredients and formulations, was placed on a diamond crystal and compressed with the instrument's knob. The spectra were recorded three times for each sample, spanning a wave number range of 400–4000 cm^{-1}.

Spreadibility studies

The spreadability of the nanoemulsion gel (NEMG) was evaluated using a "Drag & Slip" device, following a slightly modified method based on Ali et al. (2020) (Ali et al., 2020). The device consisted of a wooden block with a pulley at one end and two identical glass slides—one fixed and one movable. To conduct the test, 2.0 g of the nanoemulsion gel was placed between the stationary slide and the movable top slide. A weight of 50 g was placed on the top slide, and the time taken for the movable slide to travel a distance of 8 cm was measured, providing data on the spreadability of the gel. The following formulas were used to calculate the test NEMG's spreadibility.

$S = M \times L \div T$

In this case, S stands for Spreadibility.

"M" indicates the weight on the upper glass slide.

"L" displays the length of the glass slides, while "T" indicates how long they move.

***In vitro* drug release study**

The in vitro drug release study was performed according to a modified version of the procedure outlined by Khan et al. (2021) (Khan et al., 2021). A Franz diffusion cell (IPS Technologies, India) with a donor compartment of 6 ml and a receptor compartment of 3 ml was used for the experiment. The temperature was maintained at 37°C ± 1°C, with a stirring speed of 300 rpm throughout the process. Nanoemulsion (NEM) and nanoemulsion gel (NEMG) samples were introduced into the system. A tuffryn membrane (Sartorius, Germany) was positioned between the donor and receptor compartments to simulate the artificial barrier for in vitro release. Two grams of each formulation were added to the receptor compartments, which were filled with sodium acetate buffer at pH 5.5. Samples (2 ml) were collected from the receptor compartment at predetermined intervals (0 h, 1 h, 2 h, 4 h, 8 h, and 12 h) using a spinal syringe. After each collection, an equal amount of fresh buffer was added to the receptor compartment to maintain the buffer level and the sink condition. The drug release behaviour of the samples was analysed using a UV spectrophotometer at a wavelength of 360 nm.

Mathematical modelling: Drug release kinetics

The drug release kinetics of the nanoemulsion (NEM) and nanoemulsion gel (NEMG) formulations were analyzed to better understand the mechanism of drug release. Several mathematical models were employed, including zero-order, first-order, Higuchi, and Korsmeyer-Peppas models. The zero-order kinetic model, which represents a constant rate of drug release independent of drug concentration, was evaluated by plotting the cumulative percentage of drug release against time. First-order kinetics, assuming that the release rate depends on the remaining drug concentration, involved plotting the logarithm of the cumulative percentage of drug remaining versus time. To further explore the mechanism, the Higuchi model, which is based on Fickian diffusion and correlates drug release to the square root of time, was applied by plotting the cumulative percentage of drug released against the square root of time. Additionally, the Korsmeyer-Peppas model was used to determine the specific release mechanism, where the logarithm of cumulative drug release was plotted against the logarithm of time. The release exponent (n) from this model helped identify whether the drug release followed Fickian diffusion, non-Fickian behavior, or case II transport. For each model, the correlation coefficients (R^2) were calculated to determine the best fit for the drug release data. This analysis allowed for a detailed understanding of the release patterns, providing insights into the controlled release properties of the formulations and their potential for sustained drug delivery (Burki et al., 2020).

Inoculum Preparation for Antifungal Susceptibility Testing

The antifungal potential of the formulations was assessed through biological screening against selected fungal strains, following the method described by Motedayen et al. (2018) (Motedayen et al., 2018). Mature fungal colonies grown on Potato Dextrose Agar (PDA) were exposed to a sterile saline solution (0.85%) containing one drop of Tween 20 to ensure even distribution across the colony surface. The surface of the colonies was then gently scraped using a sterile swab to collect a mixture of conidia and hyphal fragments. This mixture was transferred to a sterile tube and allowed to settle for 5 to 10 minutes at room temperature to facilitate the sedimentation of larger particles. After this settling period, the upper suspension, which predominantly contained conidia, was carefully extracted. The conidia concentration was determined using a hemacytometer, and the suspension was adjusted using RPMI 1640 medium. The RPMI 1640 medium, which included glutamine and was buffered to pH 7.0 without sodium bicarbonate, was used to standardize the inoculum to a concentration between 1×10^3 and 3×10^3 colony-forming units per milliliter (CFU/mL). To prepare the medium, 10.43 grams of RPMI powder and 34.53 grams of MOPS buffer (N-Morpholino Propanesulfonic Acid) were dissolved in 1 liter of distilled water with continuous gentle stirring (Motedayen et al., 2018).

Minimum Inhibitory Concentration

The Minimum Inhibitory Concentration (MIC) was determined to evaluate the lowest concentration of the formulations required to inhibit visible fungal growth. The MIC was measured using the broth microdilution method, as outlined by the Clinical and Laboratory Standards Institute (CLSI). Serial dilutions of the formulations were prepared in RPMI 1640 medium, with concentrations ranging from high to low. Each dilution was placed in a 96-well microtiter plate, followed by the addition of the standardized fungal inoculum (1×10^3 to 3×10^3 CFU/mL). The plates were then incubated at 35°C for 48 hours. After the incubation period, the wells were visually inspected for fungal growth. The MIC was defined as the lowest concentration of the formulation that completely inhibited visible growth compared to the

control wells. The results of this test provided valuable insights into the antifungal efficacy of the formulations and helped guide the optimization of their antifungal properties (Kataki, 2010, Kataki et al., 2010, Mukherjee et al., 1995, Motedayen et al., 2018).

Statistical analysis

The data obtained from the experiments were subjected to statistical analysis to ensure accuracy and reliability. All experiments were conducted in triplicate, and the results were expressed as mean ± standard deviation (SD). To determine the significance of differences between groups, one-way analysis of variance (ANOVA) was employed, followed by post-hoc tests such as Tukey's test for multiple comparisons. A p-value of less than 0.05 was considered statistically significant. Statistical calculations were performed using appropriate software, such as GraphPad Prism to analyze the results. This approach ensured that the differences observed in drug release, antifungal activity, and other experimental parameters were statistically validated, providing confidence in the study's conclusions.

RESULTS & DISCUSSION

Characterizations

Thermodynamic stability and physical evaluation

Over 28 days, three formulations—blank formulations, chitosan-based nanoemulsion gel, and eucalyptus oil nanoemulsion—were stored at different conditions (8°C, 25°C, 40°C, and 40°C with 75% relative humidity). Physical evaluations were periodically performed to assess phase separation, consistency, liquefaction, color changes, and cracking. Initially, the formulations had a yellowish hue and a smooth, elegant texture. No phase separation occurred after centrifugation at 6000 and 12000 rpm. The pH of the freshly prepared formulations was 5.5, which was compared with the normal pH of human skin for reference (Proksch, 2018). The pH of the formulations was measured at intervals of 12 hours, 24 hours, 7 days, 14 days, 1 month, 2 months, and 3 months. No significant differences in pH were observed across these time points ($p > 0.05$), as determined by the Student's t-test. For topical applications, it is important to maintain a pH between 5 and 6 to prevent skin irritation (Proksch, 2018, Wagner et al., 2003). Although a gradual drop in pH was noted over time, possibly due to water loss or the formation of acidic compounds from the oils, the pH remained within the normal range for human skin. Despite these minor fluctuations, all formulations demonstrated thermodynamic stability (Wagner et al., 2003, Schmid-Wendtner and Korting, 2006)..

Polydispersity (PDI), Droplet size and surface charge

The data on zeta potential, droplet size, and polydispersity index (PDI) for the formulations provide insights into their stability and size distribution. The blank formulation (F1) has a droplet size of 57.45 nm, a zeta potential of -23.6 mV, and a PDI of 0.146, indicating a relatively stable formulation with uniform droplet distribution. The nanoemulsion (F2) shows a slightly larger droplet size of 72.84 nm and a zeta potential of -20.8 mV, suggesting good stability, with a PDI of 0.137, reflecting uniformity similar to the blank formulation.

The nanogel (F3), however, has a larger droplet size of 85.73 nm and a positive zeta potential of 24.7 mV, indicating a different charge profile compared to the other two formulations. The PDI of 0.378 for F3 is higher, suggesting less uniformity in droplet size distribution compared to F1 and F2. Overall, F1 and F2 exhibit good stability and uniformity, while F3, though stable, may have greater variability in droplet size (Rai et al., 2018, Zhang, 2019, Chakraborty et al., 2020).

Table 2. Zeta potential, PDI, and droplet size of the formulations

Prepared Formulations	Size of droplets (nm)	Zeta potential (Mv)	PDI Ratio
F1 - Blank	57.45±1.12	-23.6	0.146
F2 – Nanoemulsion (NEM)	72.84±1.09	-20.8	0.137
F3 – Nanogel (NEMG)	85.73±1.33	24.7	0.378

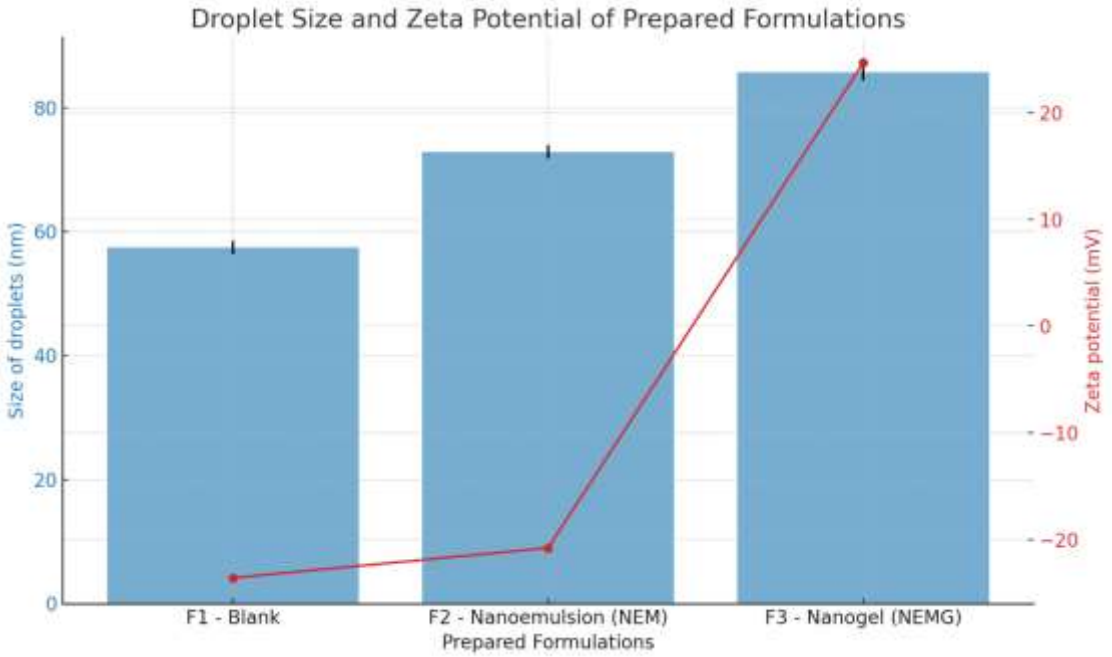

Figure 1. Zeta potential and droplet size of the formulations

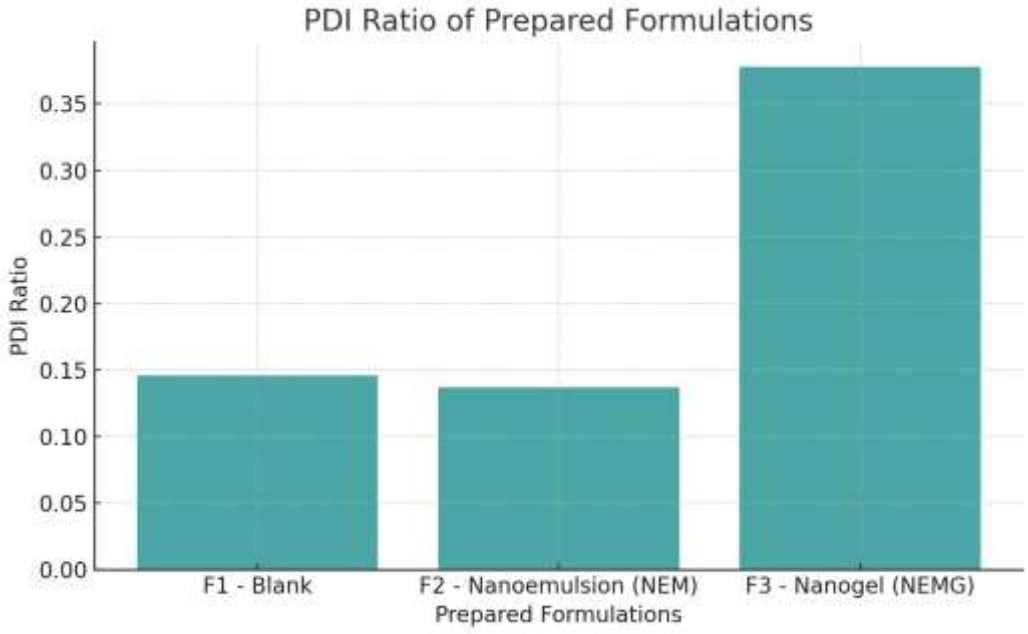

Figure 2. PDI Ratio of the formulations

FTIR study

The FTIR spectroscopy analysis was conducted to investigate any potential interactions between the drug and excipients in the prepared formulations. The spectra of the individual components, including the drug, chitosan, and other formulation constituents, were compared with those of the final formulations, such as the nanoemulsion and nanogel. The characteristic absorption peaks of the functional groups in the drug and excipients were observed in the FTIR spectra without any significant shifts or disappearance of peaks. This indicated that the chemical structure of the drug remained intact and no interaction occurred between the drug and the excipients. The key functional groups, including O-H, C=O, and N-H stretching, were clearly present in both the individual components and the formulations, further supporting the absence of any chemical bonding or interaction between the drug and the polymer matrix. The stability of these functional groups within the nanoemulsion and nanogel formulations suggests that the integrity of the drug and excipients was preserved during the formulation process. This confirms that the prepared formulations are compatible, with no evidence of chemical interaction that could affect the drug's efficacy or stability, making the formulations suitable for further development and use (Pant et al., 2014, Cardenas and Miranda, 2004).

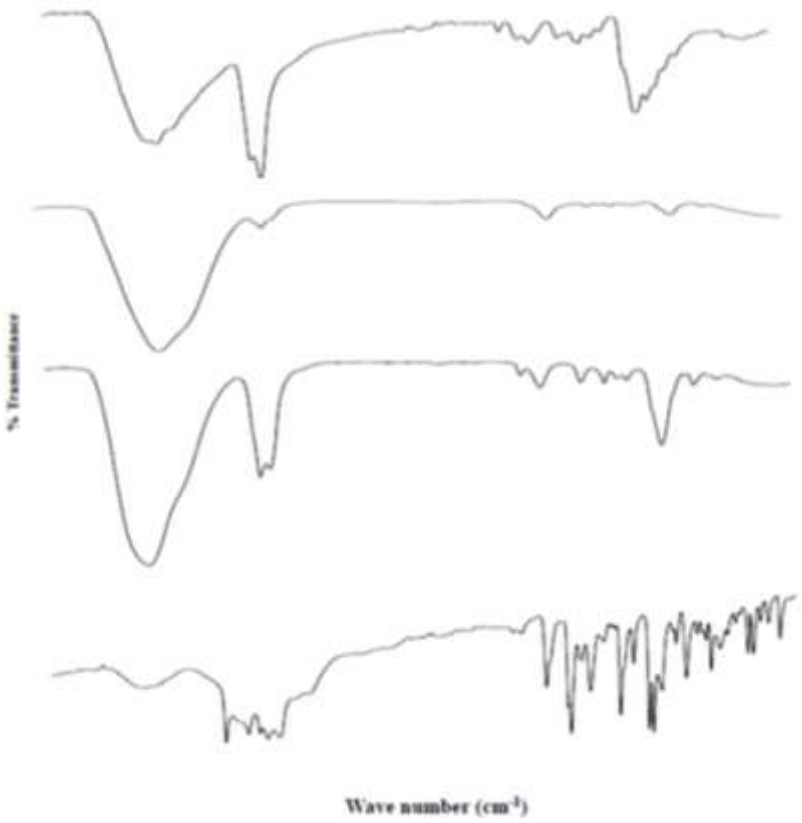

Figure 3. FTIR spectra of the drug, the olive oil-containing nanoemulsion, the chitosan, and the nanogel

Drug content analysis

The drug content data from Table 3 compares formulations F2 and F3, both containing 2% w/w of the drug. Formulation F2 achieved a higher drug content of 94.79% ± 1.51, indicating that almost the entire intended drug quantity was encapsulated in the nanoemulsion. Formulation

F3, on the other hand, exhibited a slightly lower drug content at 91.87% ± 1.49, though still close to the target. The minimal differences between these formulations suggest both are effective in incorporating the drug, with F2 showing a slightly more efficient drug loading. These results imply that F2 might offer a better option for maximizing drug availability, but both formulations maintain a high percentage of drug content relative to the amount required, making them suitable for therapeutic applications (Table 3).

Table 3. Displaying the drug content % in the nanoemulsion and nanogel formulations.

Formulation code	Drug Needed (% w/w)	% Drug content
F1	-	-
F2	2%	94.79±1.51
F3	2%	91.87±1.49

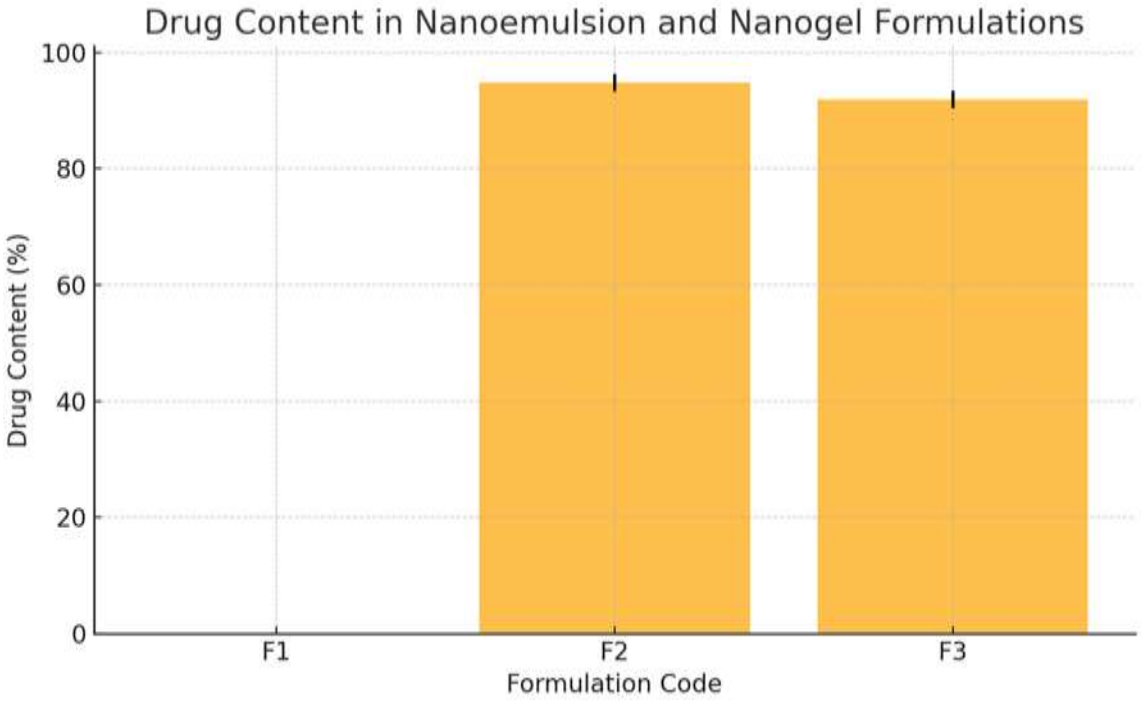

Figure 4. Drug content % in the nanoemulsion and nanogel formulations

Viscosity of formulations

Viscosity measurements of F2 (Nanoemulsion) and F3 (Nanogel) at different temperatures (8°C, 25°C, 40°C) over 28 days revealed their stability. F2 remained stable at 8°C and 25°C, with minor fluctuations, but showed a significant decrease in viscosity at 40°C, indicating temperature-induced changes, likely due to emulsion breakdown or evaporation. In contrast, F3 displayed greater variability. At 8°C, its viscosity increased slightly, while at 25°C and 40°C, fluctuations were more pronounced, particularly with a drop on Day 7 at 40°C. These changes suggest that F3 is more sensitive to environmental conditions. F2 is more suitable for temperatures up to 25°C, while F3 may require controlled environments to maintain stability or could be used in applications where viscosity variations are acceptable. Further optimization could improve F2's thermal stability and reduce F3's sensitivity to temperature changes (Khan et al., 2021, Alexander et al., 2013, Burki et al., 2020, El-Refaie et al., 2015).

Scanning electron microscopy (SEM) Study

The SEM images (Figure 5) depicted the morphology under Scanning Electron Microscopy (SEM). This image A showed a more dispersed or granular texture, indicating a porous or particle-based structure. Such morphologies are common in nanoemulsion or nanoparticle formulations, where the spherical or irregular particles are distributed evenly, reflecting a well-prepared sample with minimal aggregation. This image B presented a more fibrous or layered appearance, possibly indicating a gel or matrix-based structure. The visible fibers could suggest a strong polymer network, which is characteristic of nanogels. This fibrous structure can influence the material's mechanical strength and drug release properties, providing sustained release in applications.

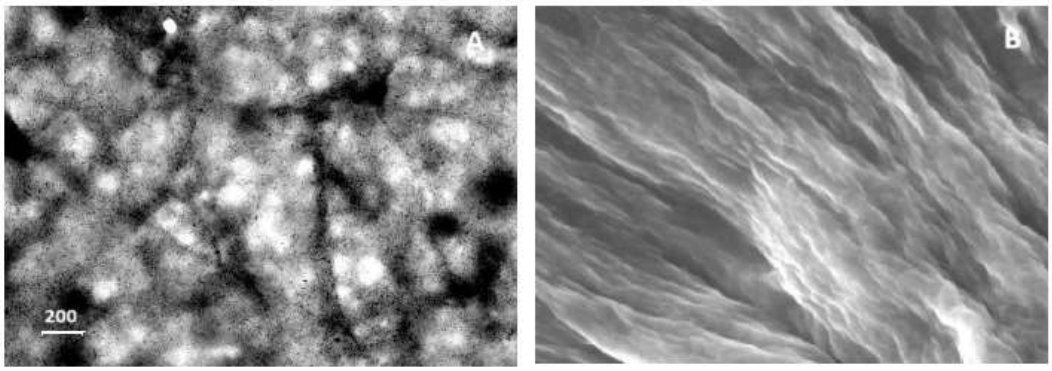

Figure 5. SEM images of the prepared formulations A. Nanoemulsion formulation (F2) and B. Nanogel formulation (F3)

Spreadibility

The data presented in Table 4 compares the spreadability of three different formulations (F1, F2, and F3) at varying temperatures (8°C, 25°C, and 40°C), expressed as mean ± standard deviation (SD). At 8°C, formulations F1 and F2 have similar spreadability values (19.84±1.34 and 19.72±1.64, respectively), indicating only a slight difference between them. In contrast, F3 exhibits a significantly lower spreadability (15.78±1.22) compared to F1 and F2. At room temperature (25°C), F1 and F2 maintain comparable spreadability (23.88±1.32 and 23.93±1.23, respectively), while F3 continues to have a much lower spreadability (17.79±1.11), indicating its reduced ability to spread at this temperature. At 40°C, the spreadability of all formulations increases, as expected with higher temperature. F1 (29.97±1.11) and F2 (29.78±1.10) remain close in their spreadability values, with minimal difference between them. However, F3, while also increasing in spreadability (19.93±1.13), remains considerably lower than F1 and F2. In summary, formulations F1 and F2 exhibit similar spreadability across all temperatures, while F3 consistently shows lower spreadability at all temperature points. The lower spreadability of F3 indicates that it may have a thicker or less easily spreadable consistency compared to F1 and F2, especially at lower temperatures. This behavior could influence the application and ease of use of the formulation in different temperature environments (Burki et al., 2020, Khan et al., 2021).

Table 4. The Spreadibility for the formulations (F1, F2, and F3) at the various temperatures under investigation was shown as mean ± SD.

	Spreadibility		
Formulation codes	**8 ^{0}C**	**25 ^{0}C**	**40 ^{0}C**

F1	19.84±1.34	23.88±1.32	29.97±1.11
F2	19.72±1.64	23.93±1.23	29.78±1.10
F3	15.78±1.22	17.79±1.11	19.93±1.13

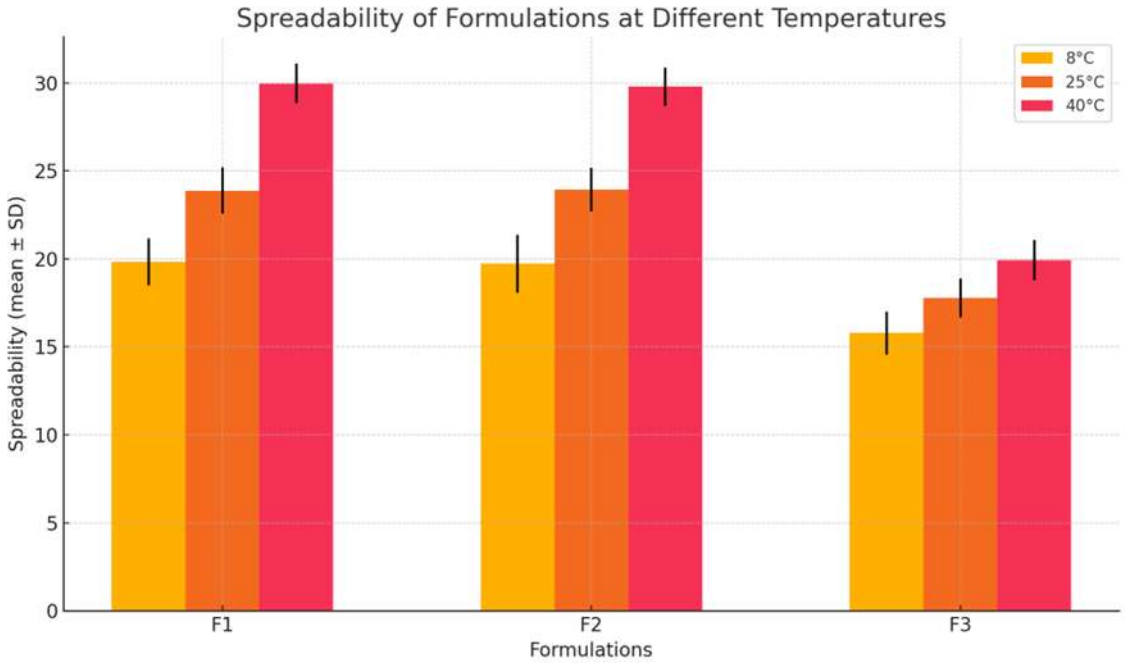

Figure 6. The Spreadability for the formulations (F1, F2, and F3) at the various temperatures.

***In vitro* drug release**

The in vitro drug release investigation comparing formulations F2 and F3 demonstrates a consistent trend in the percentage of drug release over time. At the 1-hour mark, formulation F2 released 56.84% of the drug, while F3 released slightly less at 52.84%. As the time progressed to 2 hours, F2 showed a drug release of 66.94%, continuing to surpass F3, which released 59.95%. At the 4-hour point, F2 maintained its higher release, with 75.46% compared to 70.78% for F3. By the 6-hour mark, F2 reached 81.72%, while F3 followed with 75.84%. At the final 8-hour time point, F2 released 84.84%, whereas F3 achieved 78.92%. Throughout the study, F2 consistently demonstrated a higher percentage of drug release compared to F3 at every time interval. The standard deviations reported for each data point indicate minimal variability, confirming the reliability of the results. Overall, F2 exhibited a more efficient and sustained drug release profile, making it potentially more suitable for applications requiring controlled or extended drug delivery (Burki et al., 2020, Khan et al., 2021).

Table 5. The percentage drug release data for the formulations (F2 and F3) was reported in an in vitro drug release investigation.

	Formulations	
Time (Hr)	**F2**	**F3**
0	0	0
1	56.84±2.13	52.84±1.21
2	66.94±2.31	59.95±1.19
4	75.46±2.11	70.78±1.35
6	81.72±2.14	75.84±1.61

8	84.84±2.28	78.92±1.59
12	91.49±2.42	81.88±1.87

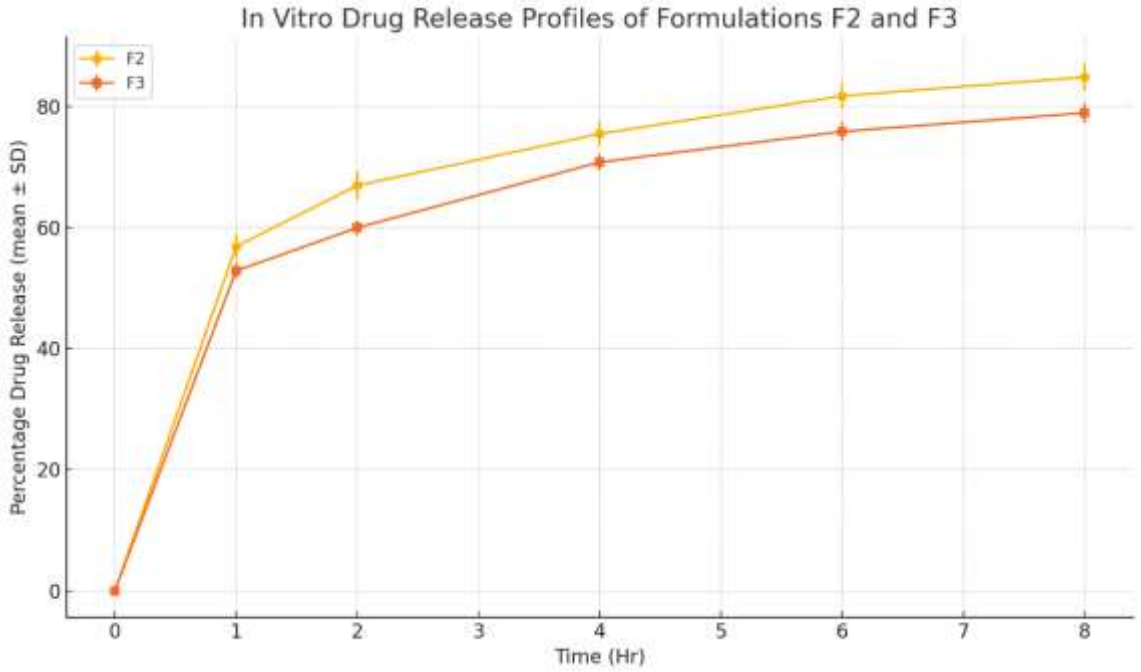

Figure 7. Illustrating the drug release % for the F2 and F3 formulations.

Antifungal Study for Susceptibility Testing

The antifungal efficacy of the nanoemulsion and nanogel formulation (NEMG, F3) was evaluated against *Trichophyton rubrum* and *Microsporum canis* strains and compared to Naftifine, a known antifungal agent. The study focused on the Minimum Inhibitory Concentration (MIC) range, MIC50 (the concentration at which 50% of strains are inhibited), and MIC90 (the concentration at which 90% of strains are inhibited) for both the NEMG formulation and Naftifine. For *T. rubrum*, Naftifine displayed an MIC range of 0.0723 to 1 µg/mL, with an MIC50 of 0.599 µg/mL and an MIC90 of 1 µg/mL. In comparison, NEMG (F3) showed enhanced antifungal activity, with a much lower MIC range of 0.0232 to 0.271 µg/mL, an MIC50 of 0.0621 µg/mL, and an MIC90 of 0.211 µg/mL. Similarly, against *M. canis*, Naftifine exhibited an MIC range of 0.0411 to 0.610 µg/mL, with an MIC50 of 0.211 µg/mL and an MIC90 of 0.581 µg/mL. NEMG (F3) again demonstrated superior antifungal efficacy with an MIC range of 0.0158 to 0.210 µg/mL, an MIC50 of 0.0322 µg/mL, and an MIC90 of 0.227 µg/mL. These results indicate that the NEMG formulation (F3) offers a more potent antifungal effect compared to Naftifine alone, with significantly reduced MIC values across both species. The enhanced activity of NEMG (F3) at lower concentrations suggests it could serve as a more effective alternative for the treatment of fungal infections caused by *T. rubrum* and *M. canis*.

Table 6. The antifungal efficacy of the nanoemulsion and nanogel formulations against strains of *T. rubrum* and *M. canis* was evaluated in comparison to Naftifine alone.

Species/Antifungal Agent	**MIC Range (µg/mL)**	**MIC50 (µg/mL)**	**MIC90 (µg/mL)**
T. rubrum (n = 50)			
Naftifine	0.0723 - 1	0.599	1

NEMG (F3)	0.0232 - 0.271	0.0621	0.211
M. canis (n = 50)			
Naftifine	0.0411 - 0.610	0.211	0.581
NEMG (F3)	0.0158 - 0.210	0.0322	0.

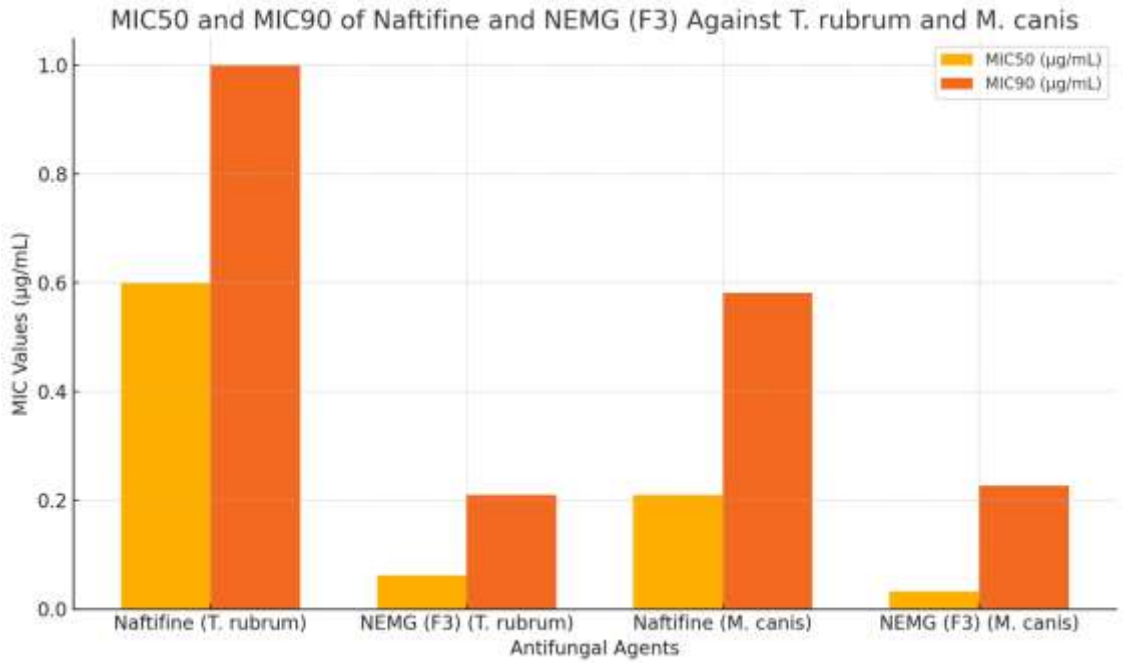

Figure 8. Comparison of the antifungal efficacy of the nanoemulsion and nanogel formulations against *T. rubrum* and *M. canis* strains with Naftifine alone

CONCLUSION

This study successfully developed and characterized nanoemulsion-based nanogels for the improved delivery of Naftifine. The nanogels demonstrated enhanced physical stability, with consistent droplet size, zeta potential, and PDI values across different formulations. Drug content analysis confirmed effective drug incorporation, and FTIR studies showed no interaction between Naftifine and the formulation excipients, ensuring chemical stability. The nanogel formulation (F3) exhibited lower spreadability compared to the nanoemulsion, indicating its thicker consistency and potential for controlled release. Importantly, F3 showed enhanced drug release and superior antifungal activity compared to the nanoemulsion alone, as evidenced by its lower MIC values against *Trichophyton rubrum* and *Microsporum canis*. These findings suggest that nanoemulsion-based nanogels could serve as a promising platform for improving the therapeutic efficacy of antifungal agents like Naftifine, particularly for sustained or localized drug delivery applications. Further studies could optimize these formulations for clinical use in the treatment of fungal infections.

DECLARATION OF INTEREST

None

FUNDING

Nil

REFERENCE

1. ALEXANDER, A., KHICHARIYA, A., GUPTA, S., PATEL, R. J., GIRI, T. K. & TRIPATHI, D. K. 2013. Recent expansions in an emergent novel drug delivery technology: Emulgel. *Journal of Controlled Release,* 171**,** 122-132.
2. ALI, M., KHAN, N. R., BASIT, H. M. & MAHMOOD, S. 2020. Physico-chemical based mechanistic insight into surfactant modulated sodium Carboxymethylcellulose film for skin tissue regeneration applications. *Journal of Polymer Research,* 27**,** 1-11.
3. BALFOUR, J. A. & FAULDS, D. 1992. Terbinafine: a review of its pharmacodynamic and pharmacokinetic properties, and therapeutic potential in superficial mycoses. *Drugs,* 43**,** 259-284.
4. BURKI, I. K., KHAN, M. K., KHAN, B. A., UZAIR, B., BRAGA, V. A. & JAMIL, Q. A. 2020. Formulation development, characterization, and evaluation of a novel dexibuprofen-capsaicin skin emulgel with improved in vivo anti-inflammatory and analgesic effects. *AAPS PharmSciTech,* 21**,** 1-14.
5. CARDENAS, G. & MIRANDA, S. P. 2004. FTIR and TGA studies of chitosan composite films. *Journal of the Chilean Chemical Society,* 49**,** 291-295.
6. CHAKRABORTY, M., HASANUZZAMAN, M., RAHMAN, M., KHAN, M. A. R., BHOWMIK, P., MAHMUD, N. U., TANVEER, M. & ISLAM, T. 2020. Mechanism of plant growth promotion and disease suppression by chitosan biopolymer. *Agriculture,* 10**,** 624.
7. DARKES, M. J. M., SCOTT, L. J. & GOA, K. L. 2003. Terbinafine: a review of its use in onychomycosis in adults. *American journal of clinical dermatology,* 4**,** 39-65.
8. DAS, A., BANERJEE, S., RAZA, S., CHATTERJEE, S. & SENGUPTA, S. 2024. Naftifine, an effective therapeutic option in limited variety of tinea corporis and cruris: observations from an open label randomized controlled trial. *Clin Exp Dermatol*.
9. DONTHI, M. R., MUNNANGI, S. R., KRISHNA, K. V., MARATHE, S. A., SAHA, R. N., SINGHVI, G. & DUBEY, S. K. 2022. Formulating Ternary Inclusion Complex of Sorafenib Tosylate Using β-Cyclodextrin and Hydrophilic Polymers: Physicochemical Characterization and In Vitro Assessment. *AAPS PharmSciTech,* 23**,** 254.
10. EL-REFAIE, W. M., ELNAGGAR, Y. S. R., EL-MASSIK, M. A. & ABDALLAH, O. Y. 2015. Novel curcumin-loaded gel-core hyaluosomes with promising burn-wound healing potential: development, in-vitro appraisal and in-vivo studies. *International journal of pharmaceutics,* 486**,** 88-98.
11. JESSUP, C. J., GHANNOUM, M. A. & RYDER, N. S. 2000. An evaluation of the in vitro activity of terbinafine. *Medical Mycology,* 38**,** 155-159.
12. KATAKI, M. S. 2010. Antibacterial activity, in vitro antioxidant activity and anthelmintic activity of ethanolic extract of Ananas comosus L. tender leaves. *Pharmacology online,* 2**,** 308-319.
13. KATAKI, M. S., SHARMA, N., KUMAR, S., YADAV, S. & RAJKUMARI, A. 2010. Antibacterial activity, in vitro antioxidant activity and anthelmintic activity of methanolic extract of Plumbago zeylanica L. Leaves. *Journal of Pharmacy Research,* 3**,** 2908-2912.
14. KAUR, A., GABRANI, R. & DANG, S. 2019. Nanoemulsions of green tea catechins and other natural compounds for the treatment of urinary tract infection: antibacterial analysis. *Advanced pharmaceutical bulletin,* 9**,** 401.
15. KAUR, A., GUPTA, S., TYAGI, A., SHARMA, R. K., ALI, J., GABRANI, R. & DANG, S. 2017. Development of nanoemulsion based gel loaded with phytoconstituents for the

treatment of urinary tract infection and in vivo biodistribution studies. *Advanced pharmaceutical bulletin,* 7**,** 611.
16. KHAN, B. A., ASMAT, Y., KHAN, T. H., QAYUM, M., ALSHAHRANI, S. M., MENAA, F. & KHAN, M. K. 2021. Novel insight into potential leishmanicidal activities of transdermal patches of nigella sativa: formulation development, physical characterizations, and in vitro/in vivo assays. *ASSAY and Drug Development Technologies,* 19**,** 339-349.
17. KOTHAPALLI, L., OZARKAR, R., MODAK, P., DESHKAR, S. & THOMAS, A. 2024. Preparation and Evaluation of Nanoemulgel with Seed Oils for Skin Care. *Current Nanomedicine (Formerly: Recent Patents on Nanomedicine),* 14**,** 73-83.
18. KRISHNAN-NATESAN, S. 2009. Terbinafine: a pharmacological and clinical review. *Expert opinion on pharmacotherapy,* 10**,** 2723-2733.
19. LEYDEN, J. 1998. Pharmacokinetics and pharmacology of terbinafine and itraconazole. *Journal of the American Academy of Dermatology,* 38**,** S42-S47.
20. MOTEDAYEN, N., HASHEMI, S. J., REZAEI, S. & BAYAT, M. 2018. In-Vitro Evaluation of Antifungal Activity of Terbinafine and Terbinafine Nano-Drug Against Clinical Isolates of Dermatophytes. *Jundishapur J Microbiol,* 11**,** e62351.
21. MUKHERJEE, P., BALASUBRAMANIAN, R., SAHA, K., SAHA, B. & PAL, M. 1995. Antibacterial efficiency of Nelumbo nucifera (Nymphaeaceae) rhizomes extract.
22. NEWLAND, J. G. & ABDEL-RAHMAN, S. M. 2009. Update on terbinafine with a focus on dermatophytoses. *Clinical, cosmetic and investigational dermatology***,** 49-63.
23. PANT, M., DUBEY, S., PATANJALI, P. K., NAIK, S. N. & SHARMA, S. 2014. Insecticidal activity of eucalyptus oil nanoemulsion with karanja and jatropha aqueous filtrates. *International biodeterioration & biodegradation,* 91**,** 119-127.
24. PATIL, A. S., CHOUGALE, S. S., KOKATANR, U., HULYALKAR, S., HIREMATH, R. D., JAPTI, V. & MASAREDDY, R. 2024. Formulation and evaluation of itraconazole-loaded nanoemulgel for efficient topical delivery to treat fungal infections. *Therapeutic Delivery*.
25. PROKSCH, E. 2018. pH in nature, humans and skin. *The Journal of dermatology,* 45**,** 1044-1052.
26. RAI, V. K., MISHRA, N., YADAV, K. S. & YADAV, N. P. 2018. Nanoemulsion as pharmaceutical carrier for dermal and transdermal drug delivery: Formulation development, stability issues, basic considerations and applications. *Journal of controlled release,* 270**,** 203-225.
27. RANJBAR, R., ZARENEZHAD, E., ABDOLLAHI, A., NASRIZADEH, M., FIROOZIYAN, S., NAMDAR, N. & OSANLOO, M. 2023. Nanoemulsion and nanogel containing Cuminum cyminum L essential oil: antioxidant, anticancer, antibacterial, and antilarval properties. *Journal of Tropical Medicine,* 2023.
28. SCHMID-WENDTNER, M. H. & KORTING, H. C. 2006. The pH of the skin surface and its impact on the barrier function. *Skin pharmacology and physiology,* 19**,** 296-302.
29. SMOLEŃSKI, M., KAROLEWICZ, B., GOŁKOWSKA, A. M., NARTOWSKI, K. P. & MAŁOLEPSZA-JARMOŁOWSKA, K. 2021. Emulsion-based multicompartment vaginal drug carriers: from nanoemulsions to nanoemulgels. *International Journal of Molecular Sciences,* 22**,** 6455.
30. SZUMAŁA, P. & MACIERZANKA, A. 2022. Topical delivery of pharmaceutical and cosmetic macromolecules using microemulsion systems. *Int J Pharm,* 615**,** 121488.

31. WAGNER, H., KOSTKA, K.-H., LEHR, C.-M. & SCHAEFER, U. F. 2003. pH profiles in human skin: influence of two in vitro test systems for drug delivery testing. *European journal of pharmaceutics and biopharmaceutics,* 55**,** 57-65.
32. ZHANG, L. 2019. Pharmacokinetics and drug delivery systems for puerarin, a bioactive flavone from traditional Chinese medicine. *Drug Delivery,* 26**,** 860-869.
33. ZHOU, L. J., LI, F. R., HUANG, L. J., YANG, Z. R., YUAN, S. & BAI, L. H. 2016. Antifungal Activity of Eucalyptus Oil against Rice Blast Fungi and the Possible Mechanism of Gene Expression Pattern. *Molecules,* 21.